

Expression of matrix Gla protein and osteocalcin in the developing tibial epiphysis of mice

Hongrui Liu^{1*}, Jie Guo^{1*}, Shanliang Wei², Shengyu Lv¹, Wei Feng¹, Jian Cui¹, Tomoka Hasegawa³, Hiromi Hongo³, Yang Yang⁴, Xiangzhi Li⁴, Kimimitsu Oda⁵, Norio Amizuka³ and Minqi Li¹

¹Department of Bone Metabolism, School of Stomatology Shandong University, Shandong Provincial Key Laboratory of Oral Biomedicine, Jinan, China ²Department of Oral and Maxillofacial Surgery, College of Stomatology Guangxi Medical University, Nanning, China ³Department of Developmental Biology of Hard Tissue, Graduate School of Dental Medicine, Hokkaido University, Sapporo, Japan, ⁴Department of Cell Biology, Shandong University Medical School, Jinan, China and ⁵Division of Biochemistry, Niigata University Graduate School of Medical and Dental Sciences, Niigata, Japan

*These authors equally contributed to this article.

Summary. This study aimed to investigate the expression of matrix Gla protein (MGP) and osteocalcin (OCN) in the tibial epiphysis of developing mice. At 1, 2, 3, and 4 weeks after birth, tibiae were removed and processed for histochemical observations and western blot analyses under anesthesia. To evaluate bone volume, the specimens were scanned with Micro CT Scanner from the articular cartilage through the growth plate, along the long axis of tibia. At 1 week after birth, OCN reactivity was faint in the region of vascular invasion, while hardly any MGP reactivity was discernible. Subsequently, MGP reactivity was seen on the cartilaginous lacunar walls of hypertrophic chondrocytes, while OCN reactivity was evenly found not only in the bone matrix, but also in the cartilaginous lacunar walls and on the bone surfaces. Furthermore, double-immunostaining clearly showed that MGP reactivity appeared closer to the cartilage matrix than OCN reactivity until postnatal week 3. Interestingly, the immunoreactivities for MGP and OCN both showed tidemarks in the articular cartilage at postnatal week 4, and MGP reactivity was more intense than OCN reactivity. Statistical analyses showed an overall upward trend in MGP and OCN expression levels during tibial epiphysis development, even though OCN was more

abundant than MGP at every time-point. Taken together, our findings suggest that the expression of MGP and OCN increased gradually in the murine developing tibial epiphysis, and the two mineral-associated proteins may occur at the same location during a particular period, but at different levels.

Key words: Matrix Gla protein, Osteocalcin, Epiphysis, Articular cartilage, Develop

Introduction

Matrix Gla protein (MGP) was first described by Price et al. (1983). After its isolation from CaCl₂/urea extracts of demineralized bovine bone matrix, the discovery that it contained five to six residues of the vitamin K-dependent amino acid, gamma-carboxyglutamic acid (Gla) led to its current naming. Further work carried out by the same group revealed that MGP was present not only in cartilage, but also in the lung, heart, and kidney (Fraser and Price 1988; Hale et al. 1988). Other reports show that MGP's main function is to inhibit vascular and cartilaginous calcification. Mori et al. examined MGP expression by means of an *in vitro* calcification model in bovine vascular smooth muscle cells, and demonstrated that the expression of the MGP gene is modulated during the development of vascular calcification (Mori et al., 1998). A recent study showed that the MGP genotype can be used as a

genomic biomarker for predicting the progression of vascular calcification (Yoshikawa et al. 2013). Regarding the effects of MGP on cartilage and bone, Barone et al. reported that selective accumulation of MGP in bone and cartilage tissues *in vitro* may be related to the development and/or maintenance of a collagenous matrix, as reflected by increases in MGP mRNA expression (Barone et al., 1991). Besides, Luo et al. demonstrated that the MGP gene serves as a marker for the chondrogenic cell lineage during mouse development, and speculated that MGP may play distinct roles during embryogenesis and growth (Luo et al., 1995). Thus far, numerous reports have mentioned that MGP modulates cartilaginous mineralization in developing bone tissues (Loeser and Wallin, 1991; Yagami et al., 1999; Cancela et al., 2001; Pinto et al., 2003; Gavaia et al., 2006; Dan et al., 2012), although correlative histomorphological evidence is still obscure.

One of the most abundant non-collagenous matrix proteins, osteocalcin (OCN), is synthesized by osteoblasts and osteocytes and subsequently deposited in the mineralizing bone (Bronckers et al., 1985; Groot et al., 1986). The peptide has multiple functions, including activating osteoblastic bone formation, being a matrix signal for recruitment and differentiation of osteoclasts, so as to regulate bone mineralization and bone turnover (Boskey et al., 1998; Ivaska et al., 2004). When trying to elucidate the ultrastructural role of Gla proteins in bone mineralization, we used warfarin, which has a primary pharmacological effect for the inhibition of microsomal vitamin K epoxide reductase and then prevents vitamin K recycling and results in vitamin K deficiency (Suttie, 1984). Our group found that warfarin-treated animals showed lower OCN content compared to controls. Ultrastructurally, scattered crystalline particles could be found in osteoid of warfarin treated animals, suggesting that OCN plays a pivotal role in the assembly of mineralized nodules (Amizuka et al., 2009). In addition, OCN exerts not only skeletal effects but also regulates energy metabolism and fat mass (Lee et al., 2007; Ferron et al., 2008). OCN also participates in the regulation of endocrine activities, such as glucose metabolism (Ferron et al., 2008, 2012). Interestingly, Oury et al. suggested that OCN may regulate murine and human fertility through a pancreas-bone-testis axis (Oury et al., 2013).

This study investigated the expression of MGP and OCN in the tibial epiphysis of developing mice. For better assessment on the process of secondary ossification, we also performed double-staining of alkaline phosphatase (ALPase) and tartrate-resistant acid phosphatase (TRAPase) and examined the newly formed trabecular bone by micro-computed tomography (micro CT) scanning.

Materials and methods

Animal and tissue preparation

Twenty-four male ICR mice (CLEA Japan Tokyo,

Japan) were used in the experiments, and were housed with water and powder diet ad libitum. All animal experiments in this study were conducted according to the Guidelines for Animal Experimentation of Hokkaido University and Shandong University. In brief, mice were anesthetized with an intraperitoneal injection of 8% chloral hydrate (400 mg/100 g body weight) and fixed with a transcardiac perfusion of 4% paraformaldehyde in 0.1 M phosphate buffer (pH 7.4) at 1, 2, 3, and 4 weeks after birth (n=6 each). Following fixation, tibiae were removed and immersed in the same fixative for an additional 12 h. After demineralization with 10% EDTA-2Na solution for 2 weeks at 4°C, specimens were dehydrated through an ascending ethanol series and embedded in paraffin for sectioning and staining.

Histochemical examinations for ALPase, OCN, MGP, and TRAPase

5- μ m thick paraffin sections were examined for ALPase, OCN, and MGP. Briefly, dewaxed paraffin sections were treated with 0.3% hydrogen peroxide for 30 min to inhibit endogenous peroxidases, and then preincubated with 1% bovine serum albumin in phosphate-buffered saline (BSA-PBS) for 20 min at room temperature to reduce non-specific binding. Sections were incubated with 1) rabbit antiserum against rat tissue-nonspecific ALPase generated by Oda et al. (1999) at a dilution of 1:200, 2) goat anti-rat OCN antibody (Biomedical Technologies Inc., Stoughton, MA, USA) at a dilution of 1:500, or 3) rabbit anti-MGP antibody (Trans Genic Inc., Kobe, Japan) at a dilution of 1:100 in BSA-PBS at room temperature for 2 h. After rinsing with PBS, the sections were incubated with horseradish peroxidase-conjugated secondary antibodies (Chemicon International Inc., Temecula, CA, USA) at a dilution of 1:100 for 1 h at room temperature. Visualization was achieved with diaminobenzidine (DAB) as the substrate. Double-staining of ALPase and TRAPase was performed as previously reported (Li et al., 2013). Staining was assessed by light microscopy, and all sections were faintly counterstained with methyl green. The primary antibody was replaced with 1 \times PBS as a negative control.

Double-staining for MGP and OCN

After the MGP-immunoreactivity was visualized by DAB-staining as described above, the same sections were incubated with a goat anti-rat OCN antibody at a dilution of 1:500 for 2 h at room temperature, followed by an ALPase-conjugated anti-rat antibody (Kirkegaard & Perry Laboratories Inc., Gaithersburg, MD, USA). For the ALPase enzyme reaction as previously reported (Li et al., 2006), the sections were dipped in a mixture of 5 mg of naphthol AS-BI phosphate (Sigma) as the substrate and 18 mg of fast blue RR salt (Sigma) diluted in 30 mL of 0.1 M Tris-HCl buffer (pH 8.5) at 37°C for 30 min. Finally, the sections were faintly counterstained

MGP and OCN in developing epiphysis

with methyl green and viewed by light microscopy.

Western blot analysis of MGP and OCN

Eight male ICR mice aged 1, 2, 3 and 4 weeks (n=2 each) were used. Immediately after sacrifice, their bilateral tibias were harvested and the diaphyses were removed. After being washed repeatedly with PBS, the retained epiphysis were placed in a sterile contusion mortar containing a grinding rod and pulverized quickly with sufficient liquid nitrogen. Pulverized tissues were homogenized in 1× RIPA Lysis Buffer (CWbio, Beijing, China), followed by protein extraction according to the manufacturer's recommended protocol.

After removal of insoluble materials by centrifugation, protein samples were diluted with 5×SDS gel loading buffer and boiled for 5 minutes. After being separated electrophoretically on a 15% SDS polyacrylamide gel, proteins were then transferred to nitrocellulose membranes. The membranes were blocked with 5% nonfat milk for 1 h and washed using TBST. Subsequently, the membranes were incubated overnight at 4°C with rabbit anti-MGP antibody (Trans Genic Inc) and goat anti-OCN antibody (Biomedical Technologies Inc) in 3% bovine serum albumin. To normalize total protein, the membranes were reprobbed with mouse anti-β-actin antibody (Applygen, Beijing, China). After three times washing, the membranes were then treated with HRP-conjugated secondary antibodies (Chemicon International Inc) for 1 h. Chemiluminescence detection was performed using chemiluminescent kit (Millipore, Billerica, MA, USA) and images were scanned with an Alpha chemiluminescence FluorChem E gel imaging system (Proteinsimple, Silicon Valley, California, USA).

Micro CT analysis

To analyze trabecular bone volume, the specimens were scanned with a Skyscan 1172 High-resolution Micro CT Scanner (Skyscan, Kontich, Belgium) from the articular cartilage through the growth plate, along the long axis of tibia (source voltage 80 kV, source current 100 μA, and image pixel size 9.8). Then, NRecon/NReconServer Reconstruction Software Package (Skyscan) and CTAN/CTVOL Software Package (Skyscan) were used for 3D reconstruction and analysis. Trabecular bone volume (BV/TV, %) was calculated to reflect the newly formed bone quantity.

Statistical analysis

Image Pro Plus 6.2 software (Media Cybernetics, Silver Spring, MD) was used for measuring cartilage tissue area and the integrated optical density of MGP and OCN reactivity in the developing epiphysis. In brief, regions of interest (ROI) were manually selected in a color cube based manner. At least 6 sections from each group were analyzed. All values are presented as means

± standard deviation. Differences among groups were assessed by unpaired Student's t-test, and considered statistically significant at p<0.05.

Results

Histological alterations in the tibial epiphysis and statistical analysis of cartilage tissue and trabecular bone volume

At 1 week after birth, the tibial epiphysis was almost completely occupied by cartilage tissue (Fig. 1A). As the beginning of secondary ossification, vascular invasion was observed at the top left corner of the epiphysis and TRAPase-positive osteoclasts were seen adjacent to the cartilage matrix in that area (Fig. 1B,C). Along with the development of secondary ossification, larger populations of ALPase-positive osteoblasts and TRAPase-positive osteoclasts were found in the tibial epiphysis, suggesting active bone remodeling (Fig. 1F,J). As a result of the bone remodeling, the epiphyseal trabeculae became thicker (Figs. 1E, I). Interestingly, the articular cartilage showed tidemarks at 4 weeks after birth (Fig. 1L). Histochemical examinations showed no ALPase and TRAPase immunoreactivities in the areas corresponding to the tidemarks, suggesting that the tidemarks were not associated with bone remodeling (Fig. 1M). Statistical analysis found significant differences in cartilage tissue volume among the groups (Table 1). Also, newly formed trabecular bone appeared significantly different among the groups (Table 1).

Immunolocalization of MGP and OCN in the developing tibial epiphysis and statistical analysis of MGP-reactivity and OCN-reactivity

At 1 week after birth, OCN-reactivity was faintly found in the region of vascular invasion, but no MGP-reactivity was discernible (Fig. 3A,B, 4A-C). In the subsequent stages, MGP-reactivity was seen on the cartilaginous lacunar walls of hypertrophic chondrocytes (Figs. 3C,E, 4D,G), while OCN-reactivity was found not only evenly in the bone matrix, but also intensely on the cartilaginous lacunar walls and bone surface (Figs. 3D,F, 4E,H). Importantly, double-staining clearly showed that

Table 1. Statistical values of cartilage tissue and trabecular bone volume in the developing tibial epiphysis.

	1 week	2 weeks	3 weeks	4 weeks
CTV	0.91±0.01	0.75±0.01*	0.66±0.01*	0.28±0.01*
TBV	6.07±0.09	12.05±0.11*	36.01±0.26*	60.18±0.98*

Data are expressed as mean±SD; p value was determined by unpaired Student's t-test. *p<0.05 with the prior point-in-time in the same group. CTV, cartilage tissue volume; TBV, trabecular bone volume.

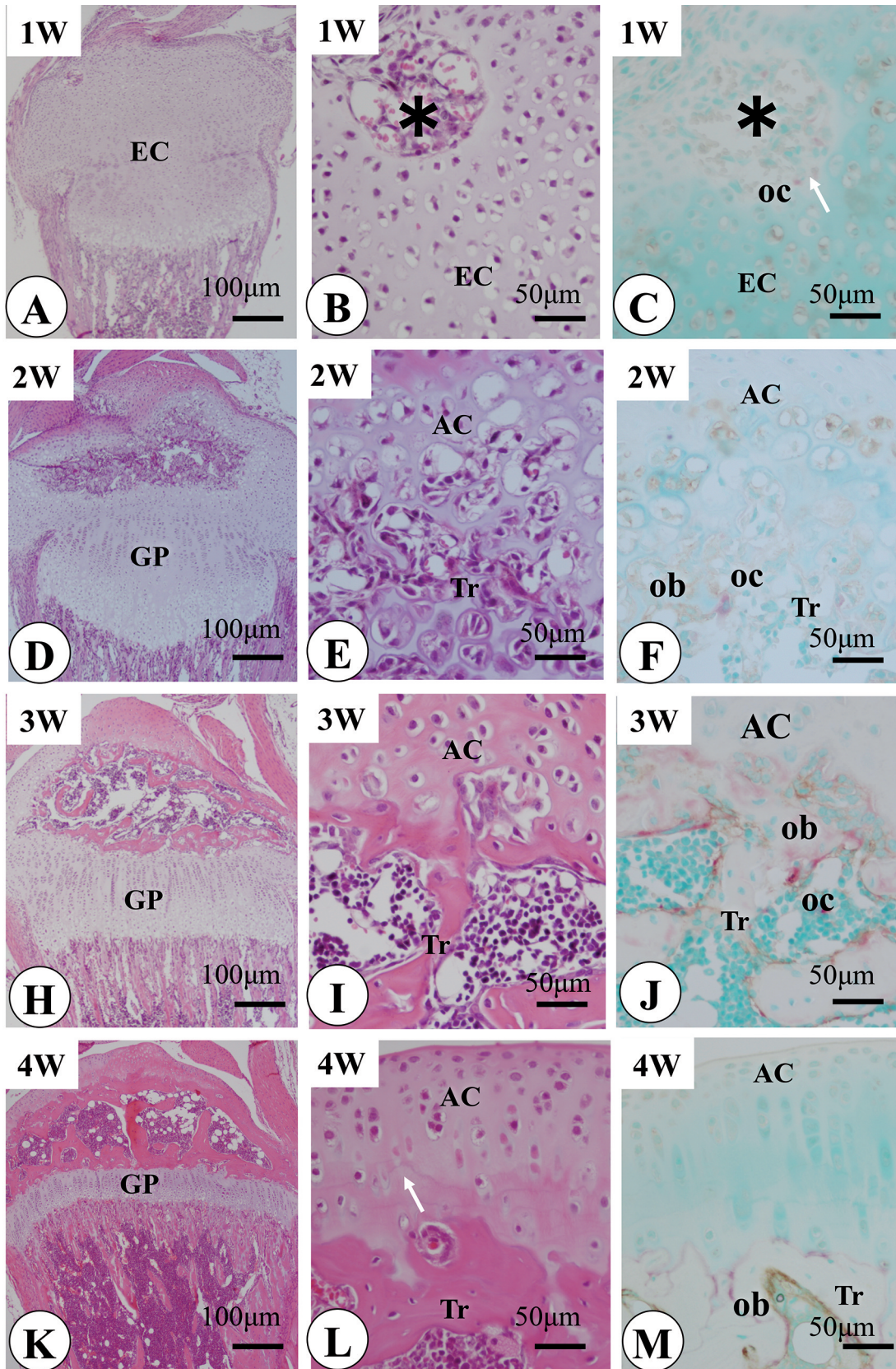


Fig. 1. Hematoxylin-eosin staining and double-staining for ALPase and TRAPase. **A, D, H, K.** Low-magnification image of the tibial epiphysis from 1 to 4 weeks after birth. **B.** High-magnification image showing a vascular invasion area (asterisk) in the tibial epiphysis at 1 week after birth. **C.** TRAPase-positive osteoclasts are seen adjacent to the cartilage matrix (white arrows) in the corresponding area to (**B**). **E.** High-magnification image of (**D**). Articular cartilage with hypertrophic chondrocytes, cartilage cores, and naïve bone trabeculae are observed in the image. **F.** Larger populations of osteoblasts (brown color) and osteoclasts (red color) are seen in the region of secondary ossification. **I.** High-magnification image of the panel in (**H**). Secondary ossification has further developed and the partition between the articular cartilage and bone trabeculae areas is much clearer. **J.** Double-staining of ALPase and TRAPase shows many ALPase-positive osteoblasts and TRAPase-positive osteoclasts. **L.** High-magnification image of the panel in (**K**). Some tidemarks are seen in the articular cartilage (white arrows). **M.** Histochemistry for ALPase and TRAPase shows no ALPase-reactivity or TRAPase-reactivity in the areas corresponding to the tidemarks. EC: epiphyseal cartilage; oc: osteoclast; ob: osteoblast; Tr: trabecula; GP: growth plate; AC: articular cartilage. Bar, A, D, H, K, 100 µm; B, C, E, F, I, J, L, M, 50 µm

MGP and OCN in developing epiphysis

MGP-reactivity was closer to the cartilage matrix than OCN-reactivity (Figs. 4F,I). At 4 weeks after birth, both MGP and OCN showed immunoreactivity at the above-mentioned tidemarks, and further examination of serial sections showed that MGP-reactivity was stronger than OCN-reactivity in these positions (Fig. 4L,M). Statistical analysis showed significant difference in MGP-reactivity and OCN-reactivity among the groups (Table 2). Specifically, both MGP and OCN reactivity were hardly detected at week-1 and increased gradually from week-2

to week-4. In addition, OCN was more abundant than MGP at every time-point (Table 2). Western blot analysis (Fig. 5) also showed an overall upward trend in MGP/OCN expression during tibial epiphysis development.

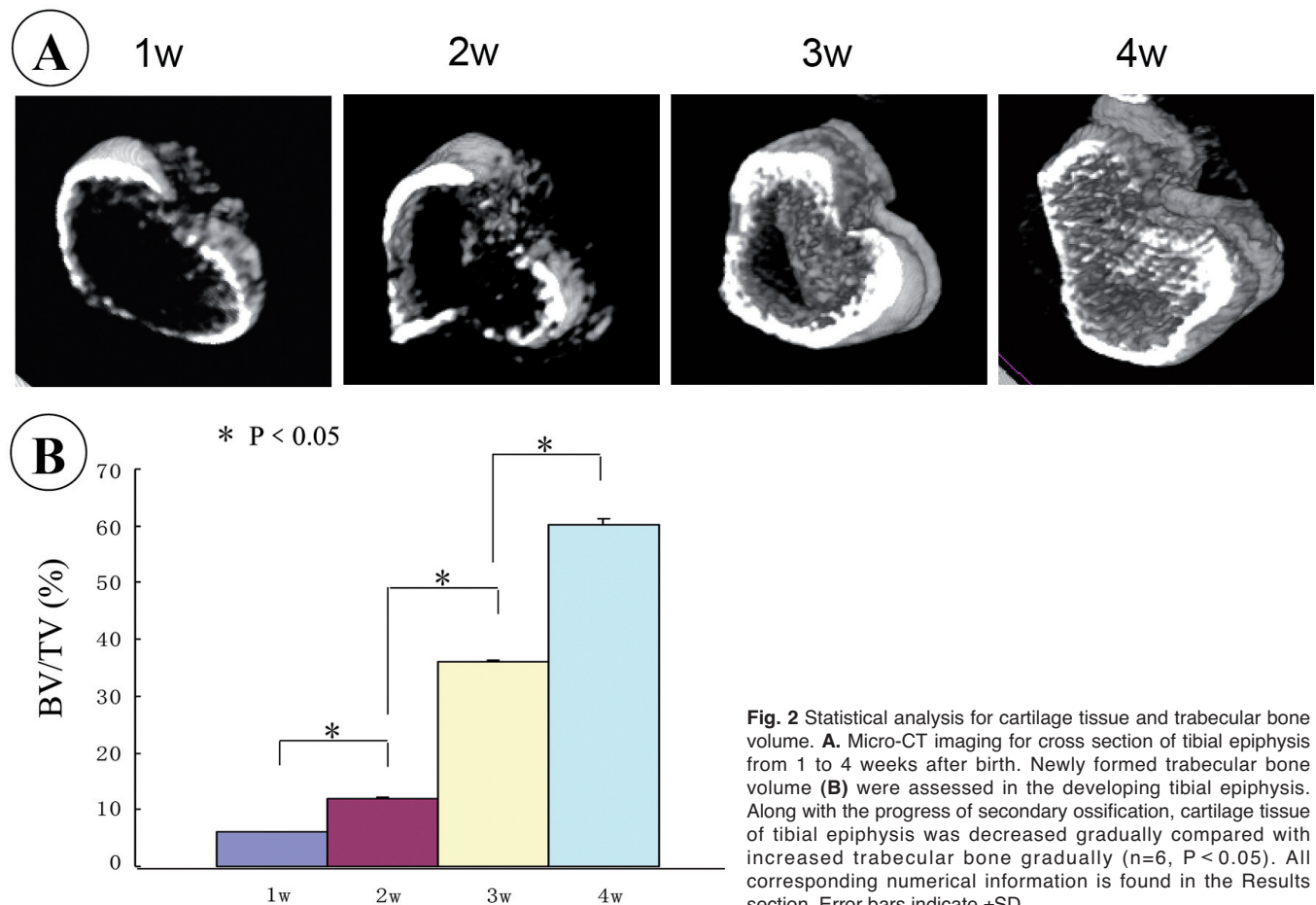
Discussion

In this study, we investigated the positional relationship between MGP and OCN in the tibial epiphysis of developing mice by immunohistochemistry. As shown in Fig. 1A,B, the tibial epiphysis was almost completely occupied by cartilage tissue and the first sign of secondary ossification was observed at postnatal week 1. At that time-point, OCN-immunoreactivity was faintly found in the initial ossification center of the tibial epiphysis, while MGP-reactivity was not detected. Our findings verified that the OCN content of vascularized mesenchymal stem cells is elevated and that MGP is expressed in the secondary ossification center just prior to calcification (Kawamura et al., 2006; Dan et al., 2012).

Table 2. Statistical values of MGP-reactivity and OCN-reactivity in the developing tibial epiphysis.

	1 week	2 weeks	3 weeks	4 weeks
MGP	-	11.91±1.06	57.31±1.44*	471.30±12.04*
OCN	-	154.13±9.82	384.63±7.91*	1996.63±13.23*

Data are expressed as mean±SD; p value was determined by unpaired Student's t-test. *p<0.05 with the prior point-in-time in the same group.



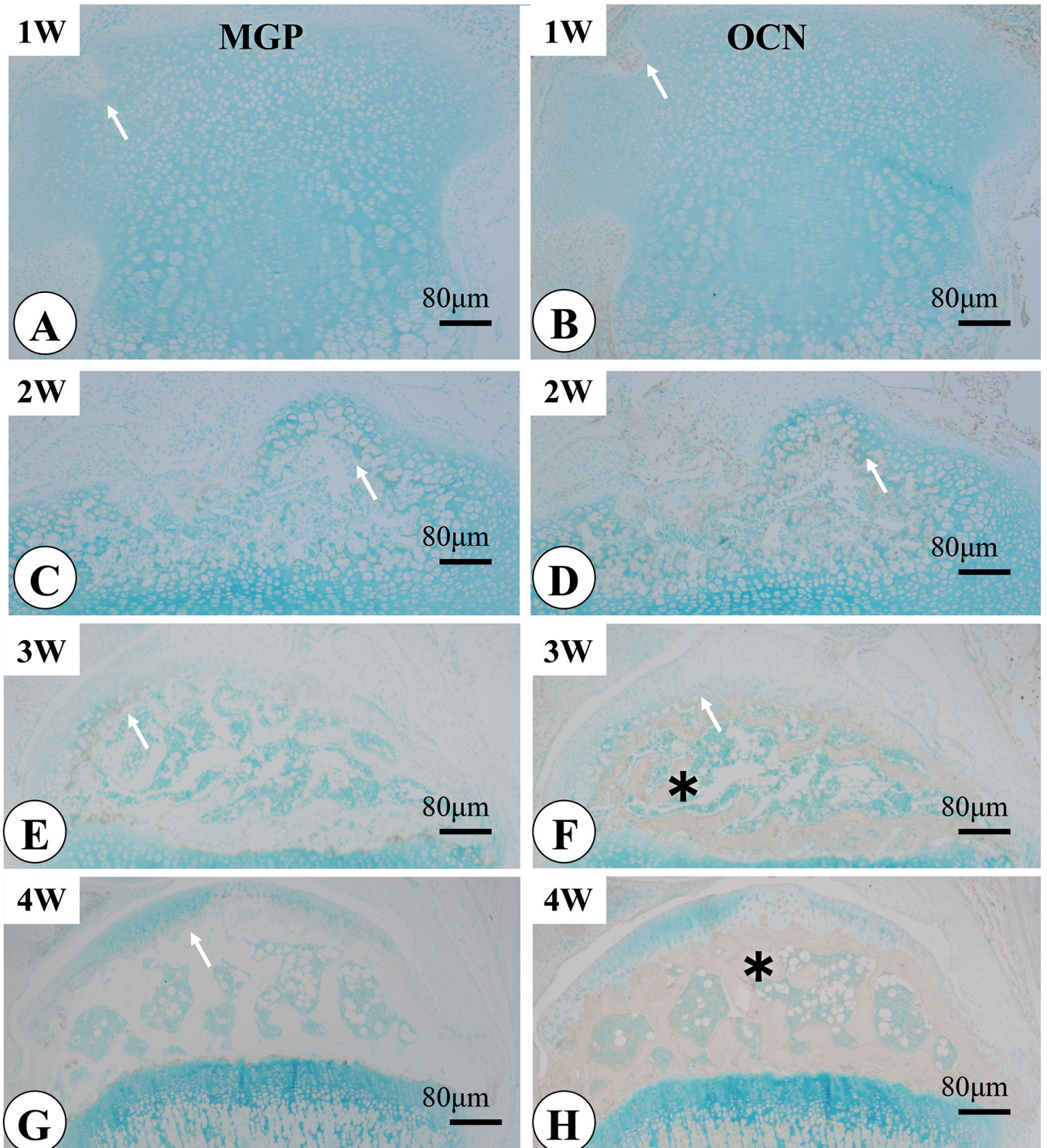


Fig. 3 Lower magnification immunolocalization of MGP and OCN. **A, C, E, G.** Immunolocalization of MGP in the developing tibial epiphysis from 1 to 4 weeks after birth. **B, D, F, H.** Immunolocalization of OCN in the corresponding areas to **(A), (C), (E)** and **(G)**, respectively. **A, B.** No immunoreactivity for MGP is discernible, but OCN-reactivity is found in the region of the vascular invasion. **C, D.** Both MGP-reactivity and OCN-reactivity are seen on the surface of the cartilage matrix, as indicated by the white arrows. **E-H.** Both MGP-reactivity and OCN-reactivity are not only seen on the surface of the cartilage matrix (white arrows), but OCN-reactivity is also detectable in the thin bone matrix surrounding the cartilage cores (asterisk). Bar, 80 μ m

MGP and OCN in developing epiphysis

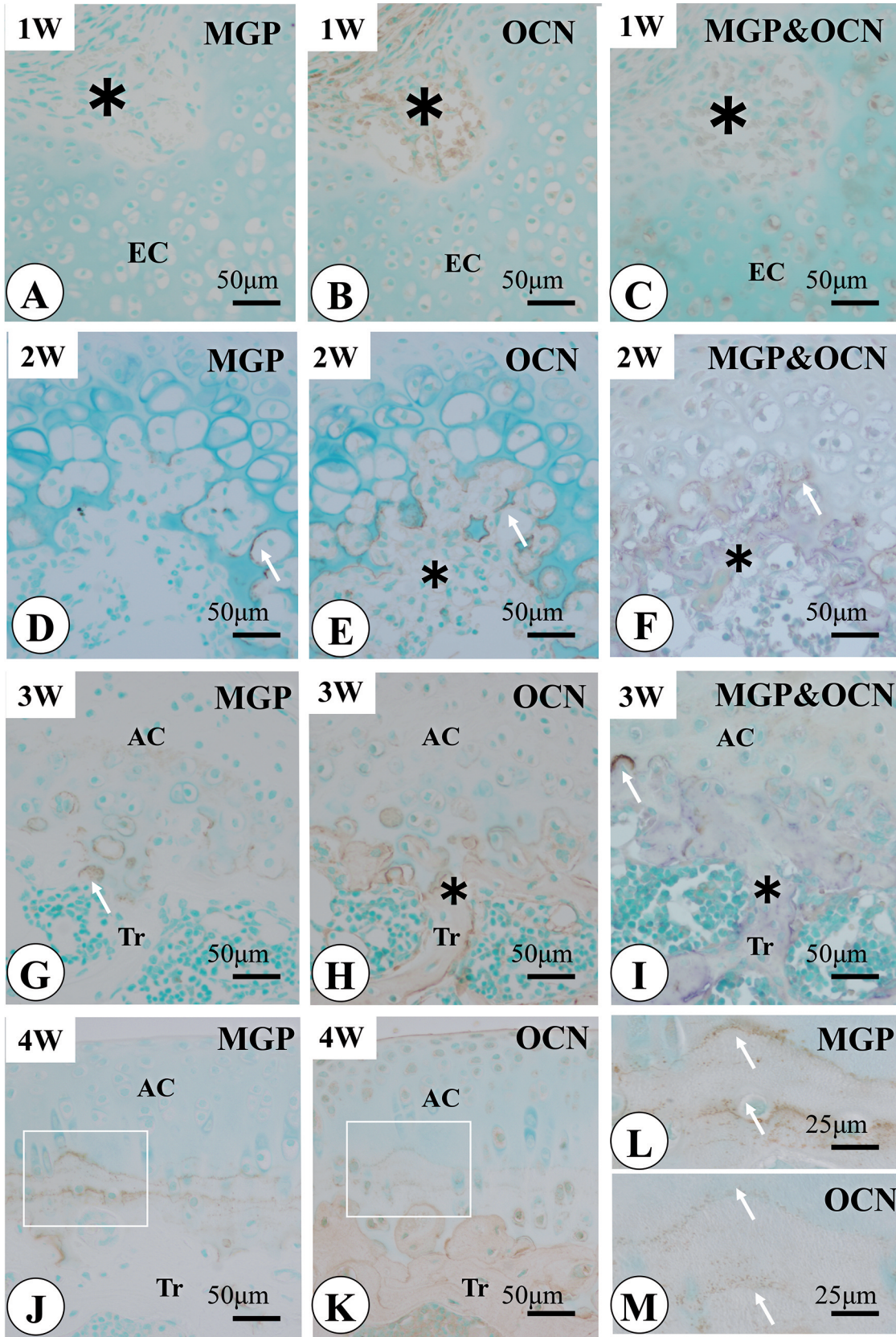


Fig. 4. Higher magnification immunolocalization of MGP and OCN. **A, D, G, J.** Immunolocalization of MGP in the developing tibial epiphysis from 1 to 4 weeks after birth. **B, E, H, K.** Immunolocalization of OCN in the corresponding areas to **(A), (D), (G) and (J)**, respectively. **C, F, I.** Double-staining for MGP and OCN in the developing tibial epiphysis from 1 to 3 weeks after birth. **L, M.** High-magnification image of the panel in **(J) and (K)**. **A-C.** Immunoreactivity for OCN (brown color in **B**; violet color in **C**) is found in the region of the vascular invasion (**B, C**), but no immunoreactivity for MGP is discernible (**A, C**). **D-F.** Both MGP-reactivity and OCN-reactivity are seen on the surface of the cartilage matrix (white arrows). Moreover, OCN-reactivity is also detectable in the thin bone matrix surrounding the cartilage cores (asterisk). Double-staining clearly shows that the MGP-reactivity is closer to the cartilage matrix than the OCN-reactivity (**F**). **G-I.** MGP is restricted to the cartilaginous lacunar walls of hypertrophic chondrocytes (**G, I**, white arrows). In contrast, OCN is seen not only evenly in the bone matrix (asterisk), but also intensely on the cartilaginous lacunar walls and bone surfaces (**H, I**). **J-M.** MGP and OCN both show immunoreactivity at the tidemarks, but MGP-reactivity is much stronger than OCN-reactivity in these areas. EC: epiphyseal cartilage; Tr: trabecula; AC: articular cartilage. Bar, A-K, 50 µm; L, M, 25 µm

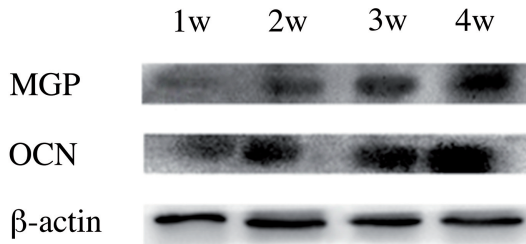


Fig. 5. Western blot analysis of MGP and OCN. Western blot analysis showed an overall upward trend in MGP/OCN expression during tibial epiphysis development. Equal loading was assessed by probing with an antibody against β -actin.

As development progressed, larger populations of ALPase-positive osteoblasts and TRAPase-positive osteoclasts appeared in the epiphysis and active bone remodeling contributed to the trabeculae becoming thicker. As the first inhibitor of calcification of arteries and cartilage to be characterized *in vivo* (Luo et al., 1997), MGP was seen on the cartilaginous lacunar walls of the hypertrophic chondrocytes, while OCN, a regulator of bone maturation (Boskey et al., 1998), was found not only evenly in the bone matrix, but also intensely on the cartilaginous lacunar walls and bone surface. Furthermore, double-staining clearly showed that the MGP-reactivity was closer to the cartilage matrix than the OCN-reactivity at postnatal weeks 2 and 3. Corresponding to these observations, and more importantly, the amount of MGP and OCN increased gradually with mineralization of the bone matrix, as shown in Table 2. These findings are consistent with a previous study, which demonstrated that OCN gene polymorphism is associated with bone mineral density (BMD), and Gla gene polymorphisms are associated with higher OCN levels (Kim et al., 2006).

Previous reports demonstrated that MGP gene expression and protein accumulation were restricted to cartilaginous or organic structures, whereas OCN gene expression and protein accumulation were localized in the mineralized structures (Pinto et al., 2003; Ortiz-Delgado et al., 2005). Specifically, Pombinbo et al. suggested the expression of MGP and OCN in a mutually exclusive manner using fish-bone-derived cell systems, in which MGP and OCN were expressed in chondrocyte and osteoblast cell lineages, respectively (Pombinbo et al., 2004). However, in the more significant histochemical data obtained in the present study, both MGP and OCN showed immunoreactivity at the tidemarks shown in the articular cartilage at 4 weeks after birth, although further examination of serial sections demonstrated that the MGP-reactivity was stronger than the OCN-reactivity in these positions. We consider that the tidemarks represent the mineralization front of articular cartilage and speculate that mineralization inhibition (MGP) and assembly of mineralized nodules (OCN) may occur at the same

location during a particular period, but at different levels. More detailed investigations of the proteins localized in the mineralization front need to be performed with immunoelectron microscopy in future studies.

In view that the abnormal MGP/OCN expression are involved in tibial dyschondroplasia, Keutel syndrome as well as declining bone quality (Hauschka et al., 1989; Munroe et al., 1999; Dan et al., 2012), we speculated that MGP and OCN are promising indicators to represent the degree of bone mineralization and may be used in the early detection of bone metabolic disease at some level. Although our findings can be an important basis to help understand the expression changes of MGP and OCN in the developing tibial epiphysis, histochemical data has limitations and further investigation is necessary.

In summary, the expression of MGP and OCN increased gradually in the murine developing tibial epiphysis, and the two mineral-associated proteins may occur at the same location during a particular period, but at different levels.

Acknowledgements. This study was partially supported by the National Nature Science Foundation of China (grant No. 81271965; 81311140173) and Specialized Research Fund for the Doctoral Program of Higher Education (grant No. 20120131110073) to Li M. The Ministry of Education, Culture, Sports, Science & Technology and Japanese Society for the Promotion of Science to Amizuka N.

References

- Amizuka N., Li M., Hara K., Kobayashi M., de Freitas P.H., Ubaidus S., Oda K. and Akiyama Y. (2009). Warfarin administration disrupts the assembly of mineralized nodules in the osteoid. *J. Electron Microsc.* (Tokyo). 58, 55-65.
- Barone L.M., Owen T.A., Tassinari M.S., Bortell R., Stein G.S. and Lian J.B. (1991). Developmental expression and hormonal regulation of the rat matrix Gla protein (MGP) gene in chondrogenesis and osteogenesis. *J. Cell Biochem.* 46, 351-365.
- Boskey A.L., Gadaleta S., Gundberg C., Doty S.B., Ducy P. and Karsenty G. (1998). Fourier transform infrared microspectroscopic analysis of bones of osteocalcin-deficient mice provides insight into the function of osteocalcin. *Bone* 23, 187-196.
- Bronckers A.L., Gay S., Dimuzio M.T. and Butler W.T. (1985). Immunolocalization of gamma-carboxyglutamic acid containing proteins in developing rat bones. *Coll. Relat. Res.* 5, 273-281.
- Cancela M.L., Ohresser M.C., Reia J.P., Viegas C.S., Williamson M.K. and Price P.A. (2001). Matrix Gla protein in *Xenopus laevis*: molecular cloning, tissue distribution, and evolutionary considerations. *J. Bone Miner. Res.* 16, 1611-1621.
- Dan H., Simsa-Maziel S., Reich A., Sela-Donenfeld D. and Monsonego-Ornan E. (2012). The role of matrix gla protein in ossification and recovery of the avian growth plate. *Front. Endocrinol. (Lausanne)*. 3, 79.
- Ferron M., Hinoi E., Karsenty G. and Ducy P. (2008). Osteocalcin differentially regulates beta cell and adipocyte gene expression and affects the development of metabolic diseases in wild-type mice. *Proc. Natl. Acad. Sci. USA* 105, 5266-5270.

MGP and OCN in developing epiphysis

- Ferron M., McKee M.D., Levine R.L., Ducy P. and Karsenty G. (2012). Intermittent injections of osteocalcin improve glucose metabolism and prevent type 2 diabetes in mice. *Bone* 50, 568-575.
- Fraser J.D. and Price P.A. (1988). Lung, heart, and kidney express high levels of mRNA for the vitamin K-dependent matrix Gla protein. Implications for the possible functions of matrix Gla protein and for the tissue distribution of the gamma-carboxylase. *J. Biol. Chem.* 263, 11033-11036.
- Gavaia P.J., Simes D.C., Ortiz-Delgado J.B., Viegas C.S., Pinto J.P., Kelsh R.N., Sarasquete M.C. and Cancela M.L. (2006). Osteocalcin and matrix Gla protein in zebrafish (*Danio rerio*) and Senegal sole (*Solea senegalensis*): comparative gene and protein expression during larval development through adulthood. *Gene Expr. Patterns* 6, 637-652.
- Groot C.G., Danes J.K., Blok J., Hoogendijk A. and Hauschka P.V. (1986). Light and electron microscopic demonstration of osteocalcin antigenicity in embryonic and adult rat bone. *Bone* 7, 379-385.
- Hale J.E., Fraser J.D. and Price P.A. (1988). The identification of matrix Gla protein in cartilage. *J. Biol. Chem.* 263, 5820-5824.
- Hauschka P.V., Lian J.B., Cole D.E. and Gundberg C.M. (1989). Osteocalcin and matrix Gla protein: Vitamin K-dependent proteins in bone. *Physiol. Rev.* 69, 990-1047.
- Ivaska K.K., Hentunen T.A., Vääräniemi J., Ylipahkala H., Pettersson K. and Väänänen H.K. (2004). Release of intact and fragmented osteocalcin molecules from bone matrix during bone resorption *in vitro*. *J. Biol. Chem.* 279, 18361-18369.
- Kawamura K., Yajima H., Ohgushi H., Tomita Y., Kobata Y., Shigematsu K. and Takakura Y. (2006). Experimental study of vascularized tissue-engineered bone grafts. *Plast. Reconstr. Surg.* 117, 1471-1479.
- Kim J.G., Ku S.Y., Lee D.O., Jee B.C., Suh C.S., Kim S.H., Choi Y.M., and Moon S.Y. (2006). Relationship of osteocalcin and matrix Gla protein gene polymorphisms to serum osteocalcin levels and bone mineral density in postmenopausal Korean women. *Menopause* 13, 467-473.
- Lee N.K., Sowa H., Hinoi E., Ferron M., Ahn J.D., Confavreux C., Dacquin R., Mee P.J., McKee M.D., Jung D.Y., Zhang Z., Kim J.K., Mauvais-Jarvis F., Ducy P. and Karsenty G. (2007). Endocrine regulation of energy metabolism by the skeleton. *Cell* 130, 456-469.
- Li M., Amizuka N., Takeuchi K., Freitas P.H.L., Kawano Y., Hoshino M., Oda K., Nozawa-Inoue K. and Maeda T. (2006). Histochemical evidence of osteoclastic degradation of extracellular matrix in osteolytic metastasis originating from human lung small carcinoma (SBC-5) cells. *Microsc. Res. Tech.* 69, 73-83.
- Li M., Hasegawa T., Hongo H., Tatsumi S., Liu Z., Guo Y., Sasaki M., Tabata C., Yamamoto T., Ikeda K. and Amizuka N. (2013). Histological examination on osteoblastic activities in the alveolar bone of transgenic mice with induced ablation of osteocytes. *Histol. Histopathol.* 28, 327-335.
- Loeser R.F. Jr and Wallin R. (1991). Vitamin K-dependent carboxylation in articular chondrocytes. *Connect. Tissue Res.* 26, 135-144.
- Luo G., D'Souza R., Hogue D. and Karsenty G. (1995). The matrix Gla protein gene is a marker of the chondrogenesis cell lineage during mouse development. *J. Bone Miner. Res.* 10, 325-334.
- Luo G., Ducy P., McKee M.D., Pinero G.J., Loyer E., Behringer R.R., and Karsenty G. (1997). Spontaneous calcification of arteries and cartilage in mice lacking matrix GLA protein. *Nature* 386, 78-81.
- Mori K., Shioi A., Jono S., Nishizawa Y. and Morii H. (1998). Expression of matrix Gla protein (MGP) in an *in vitro* model of vascular calcification. *FEBS Lett.* 433, 19-22.
- Munroe P.B., Olgunturk R.O., Fryns J.P., Van Maldergem L., Ziereisen F., Yuksel B., Gardiner R.M. and Chung E. (1999). Mutations in the gene encoding the human matrix Gla protein cause Keutel syndrome. *Nat. Genet.* 21, 142-144.
- Oda K., Amaya Y., Fukushi-Irie M., Kinameri Y., Ohsuye K., Kubota I., Fujimura S. and Kobayashi J. (1999). A general method for rapid purification of soluble versions of glycosylphosphatidylinositol-anchored proteins expressed in insect cells: an application for human tissue-nonspecific alkaline phosphatase. *J. Biochem. (Tokyo)* 126, 694-699.
- Ortiz-Delgado J.B., Simes D.C., Gavaia P., Sarasquete C. and Cancela M.L. (2005). Osteocalcin and matrix GLA protein in developing teleost teeth: identification of sites of mRNA and protein accumulation at single cell resolution. *Histochem. Cell Biol.* 124, 123-130.
- Oury F., Ferron M., Huizhen W., Confavreux C., Xu L., Lacombe J., Srinivas P., Chamouni A., Lugani F., Lejeune H., Kumar T.R., Ploton I. and Karsenty G. (2013). Osteocalcin regulates murine and human fertility through a pancreas-bone-testis axis. *J. Clin. Invest.* 123, 2421-2433.
- Pinto J.P., Conceição N., Gavaia P.J. and Cancela M.L. (2003). Matrix Gla protein gene expression and protein accumulation colocalize with cartilage distribution during development of the teleost fish *Sparus aurata*. *Bone* 32, 201-210.
- Pombinho A.R., Laize V., Molha D.M., Marques S.M. and Cancela M.L. (2004). Development of two bone-derived cell lines from the marine teleost *Sparus aurata*; evidence for extracellular matrix mineralization and cell-type-specific expression of matrix Gla protein and osteocalcin. *Cell Tissue Res.* 315, 393-406.
- Price P.A., Urist M.R. and Otawara Y. (1983). Matrix Gla protein, a new gamma-carboxyglutamic acid-containing protein which is associated with the organic matrix of bone. *Biochem. Biophys. Res. Commun.* 117, 765-771.
- Suttie J.W. (1984). Vitamin K. In: Machlin L.J. (ed). *Handbook of Vitamins*. Dekker. New York. pp 147-198
- Yagami K., Suh J.Y., Enomoto-Iwamoto M., Koyama E., Abrams W.R., Shapiro I.M., Pacifici M. and Iwamoto M. (1999). Matrix GLA protein is a developmental regulator of chondrocyte mineralization and, when constitutively expressed, blocks endochondral and intramembranous ossification in the limb. *J. Cell Biol.* 147, 1097-1108.
- Yoshikawa K., Abe H., Tominaga T., Nakamura M., Kishi S., Matsuura M., Nagai K., Tsuchida K., Minakuchi J. and Doi T. (2013). Polymorphism in the human matrix Gla protein gene is associated with the progression of vascular calcification in maintenance hemodialysis patients. *Clin. Exp. Nephrol.* 17, 882-889.